

Annual Review of Analytical Chemistry

Petroleomics: Tools, Challenges, and Developments

Diana Catalina Palacio Lozano,¹ Mary J. Thomas,^{1,2}
Hugh E. Jones,^{1,2} and Mark P. Barrow¹

¹Department of Chemistry, University of Warwick, Coventry CV4 7AL, United Kingdom;
email: M.P.Barrow@warwick.ac.uk

²Molecular Analytical Sciences Centre for Doctoral Training, University of Warwick,
Coventry CV4 7AL, United Kingdom

Annu. Rev. Anal. Chem. 2020. 13:405–30

First published as a Review in Advance on
March 20, 2020

The *Annual Review of Analytical Chemistry* is online at
anchem.annualreviews.org

<https://doi.org/10.1146/annurev-anchem-091619-091824>

Copyright © 2020 by Annual Reviews.
All rights reserved

ANNUAL
REVIEWS **CONNECT**

www.annualreviews.org

- Download figures
- Navigate cited references
- Keyword search
- Explore related articles
- Share via email or social media

Keywords

petroleomics, petroleum, environmental, mass spectrometry, data analysis

Abstract

The detailed molecular characterization of petroleum-related samples by mass spectrometry, often referred to as petroleomics, continues to present significant analytical challenges. As a result, petroleomics continues to be a driving force for the development of new ultrahigh resolution instrumentation, experimental methods, and data analysis procedures. Recent advances in ionization, resolving power, mass accuracy, and the use of separation methods, have allowed for record levels of compositional detail to be obtained for petroleum-related samples. To address the growing size and complexity of the data generated, vital software tools for data processing, analysis, and visualization continue to be developed. The insights gained impact upon the fields of energy and environmental science and the petrochemical industry, among others. In addition to advancing the understanding of one of nature's most complex mixtures, advances in petroleomics methodologies are being adapted for the study of other sample types, resulting in direct benefits to other fields.

1. INTRODUCTION

Energy sustainability and environmental protection for the provision of natural resources are now the priority of many researchers, particularly in light of meeting human development goals upon which the global economy and society depend (1). The depletion of fossil fuel reserves and the environmental impact of the petroleum industry present challenges requiring deep scientific comprehension. Crude oil and natural mixtures such as organic matter in soil and water, bio-oils, and lignin are characterized by their extraordinary chemical complexity and molecular diversity. Therefore, their composition at the molecular level cannot be determined by conventional analytical techniques. The comprehensive analysis of complex mixtures is of pivotal importance for the understanding of petroleum refining, exploration, and extraction, and the effects of this human activity on different ecosystems.

Detailed chemical and molecular compositional profiles can be obtained using mass spectrometry (MS) operating with sufficiently high resolution and mass accuracy. Therefore, ultrahigh resolution (UHR) mass spectrometers are indispensable tools for complex mixture analysis. Currently, Fourier transform ion cyclotron resonance (FTICR) mass spectrometers possess the highest performance capabilities in terms of resolution and mass accuracy, followed by Orbitraps, and multiple-pass time-of-flight (TOF) mass spectrometers (2). The improvements in UHR MS technologies and subsequent development of data analysis methods have been a crucial component in the development of the field of petroleomics, defined as the analysis of petroleum at the molecular level, to understand its properties and reactivity (3–5). Regardless of the analytical advances, a vast array of challenges and questions remain unsolved in petroleum-related research areas. In this review, we cover the recent analytical challenges, tools, and developments encountered in the analysis of complex chemical systems.

1.1. Ultrahigh Resolution Mass Spectrometry

Ultrahigh resolution mass spectrometers are indispensable tools for the analysis of complex mixtures, such as petroleum. Their performance characteristics afford detailed compositional profiles, with many thousands of unique molecular assignments obtained from a single spectrum.

1.1.1. Principles of operation. In order to be detected, a sample must be vaporized and ionized, producing gas-phase ions that can be analyzed according to their mass-to-charge ratio (m/z), where the total charge (q) is equal to the number of charges (z) multiplied by the charge of an electron (e). A mass spectrum is produced by plotting abundance (as signal intensity) against m/z . In general, a mass spectrometer consists of a sample introduction system, an ion source, an analyzer, and a detector. The combination of those systems defines the analytical capabilities (resolving power and mass accuracy) of the mass spectrometer. Here, some key concepts are briefly discussed; detailed reviews of UHR MS can be found elsewhere (2, 6–8).

To date, the sample introduction system most widely used in petroleomics is direct infusion. Some advantages of this method include minimal sample preparation, rapid analysis, and a wide number of compounds detected in a single experiment. As a consequence of the high complexity of crude oils, it is becoming increasingly common to perform offline or online separations of sample analytes prior to analysis by MS. Some of these systems include gas chromatography (GC), liquid chromatography (LC), supercritical fluid chromatography (SFC), pyrolyzer/GC, and trapped ion mobility spectrometry (TIMS), among others (3).

Ions may be produced through a number of different mechanisms. Depending on the ionization source and polarity, radical ions ($M^{+\bullet}$ or $M^{-\bullet}$), protonated $[M+H]^+$, and deprotonated $[M-H]^-$ species are typically detected in the mass spectra. Two of the most regularly used

ionization sources for petroleomics analysis include electrospray ionization (ESI) and atmospheric pressure photoionization (APPI). The remarkable softness of the ESI source makes electrospray suitable to ionize polar species with high molecular weight, which led to the title of the Nobel lecture “Electrospray Wings for Molecular Elephants” (9). In the case of APPI, a UV light source, typically a krypton discharge lamp emitting 10-eV photons, is used to ionize the sample that is commonly dissolved in a mixture of solvents that include toluene to assist the ionization of the analytes. Ionization sources are discussed further in following sections.

Once generated, ions are discriminated according to their m/z value in the mass analyzer. In FTICR MS the ions are transferred into an ion cyclotron cell (Penning trap) embedded in a constant high magnetic field (6). Orbitrap mass analyzers can be considered as variants of a Kingdon trap, where the ions oscillate around a central electrode between two outer electrodes (7). Therefore, in FTICR MS the ions with the same m/z will have a fundamental oscillation frequency (ω_c) or cyclotron frequency that depends directly on the magnitude of the magnetic field (\mathbf{B}) and is inversely proportional to the m/z (Equation 1) (6), while the frequency of the harmonic oscillations of the ions in an Orbitrap depends inversely upon the square root of the m/z value and directly to the field curvature (k) (Equation 2) (10). Note that the charge, q , shown in Equations 1 and 2, is determined by multiplying the number of charges, z , by the charge of an electron, e ; in this way, m/q is related to the measured m/z :

$$\omega_c = \frac{q\mathbf{B}}{m}, \quad 1.$$

$$\omega = \sqrt{\frac{q}{mk}}. \quad 2.$$

FTICR and Orbitrap mass spectrometers are examples of Fourier transform MS instruments (11). An image current of the ions is detected as a function of time and recorded as a composite sum of sinusoidal waves with different frequencies called free induction decay (FID) or transient (8). A Fourier transform is applied to the signal to convert to the frequency domain, followed by a calibration of the signal with respect to the m/z domain. Once the frequency domain is converted to m/z , a mass spectrum is produced.

1.1.2. Mass accuracy and resolving power. Complex natural mixtures may contain many hundreds of thousands of molecular compositions with close mass differences within clusters per nominal mass, normally extended over a wide mass range (12). Mass accuracy is important for confident assignment of individual molecular compositions within a mass spectrum. The mass error (in parts per million, ppm) is defined by Equation 3. UHR MS can achieve mass accuracy at the sub-ppm or even parts-per-billion (ppb) level (13, 14):

$$\text{Mass error} = \frac{m_{\text{experimental}} - m_{\text{theoretical}}}{m_{\text{theoretical}}} \times 10^6. \quad 3.$$

To achieve a high mass accuracy, it is also essential to resolve a peak of interest from compositions of similar m/z . For instance, a mass split of 0.1 mDa must be resolved in order to assign unique molecular compositions up to 500 Da for species containing C, H, N, O, and S (15). The mass resolving power of FTICR mass spectrometers and Orbitraps is defined according to Equations 4 and 5, respectively (2, 6).

$$R = \frac{m}{\Delta m} \propto \frac{q\mathbf{B}T}{mk}, \quad 4.$$

$$R = \frac{m}{\Delta m} \propto T \sqrt{\frac{q}{m}}, \quad 5.$$

in which k and T are a peak width constant and the acquisition time of the signal, respectively. Equations 4 and 5 illustrate that, for a chosen m/z range for an experiment, the resolving power in both instruments decreases as the m/z increases. Thus, in a traditional experiment, where a wide m/z range of compositions is detected in a single mass spectrum, the resolving power and mass accuracy decrease with m/z (6, 8). Equations 4 and 5 also show that the resolving powers of FTICR and Orbitrap instruments are proportional to acquisition time. As shown in Equation 6, the acquisition time can be increased by acquiring larger data set sizes (N) (normally in megawords such as 4 M, 8 M, and so forth) or by reducing the sampling frequency (f_s) (determined by the low m/z cutoff for detection, where lower m/z values correspond to higher frequencies:

$$T = \frac{N}{f_s}. \quad 6.$$

2. PETROLEOMICS TOOLS

2.1. Kendrick Mass Defect

With sufficient resolving power and mass accuracy, it is possible to determine the composition of complex mixtures at the molecular level. The elemental compositions define the compositional space that is the unique, characteristic signature, also called a fingerprint or profile, of the sample (12). An example of the molecular mass distribution of a crude oil can be found in **Figure 1**.

Use of Kendrick mass defect (KMD) greatly aids complex mixture analysis. The Kendrick mass scale (16) exploits the 14.01565 Da (CH_2) alkyl repeat unit to sort members of the same heteroatom class and double bond equivalents (DBE) (17) into homologous series. Examples of patterns depending upon a difference of CH_2 and H_2 can be found in **Figure 1**. The Kendrick mass and KMD can be calculated using Equations 7 and 8, respectively:

$$\text{Exact Kendrick mass} = \text{IUPAC mass} \times (14/14.01565), \quad 7.$$

$$\text{KMD} = (\text{nominal Kendrick mass} - \text{exact Kendrick mass}). \quad 8.$$

Plotting KMD against nominal Kendrick mass yields a plot with vertical separation of components, differing by heteroatom classes and DBE, and a horizontal separation based on alkylation (compositions separated by CH_2) (18). Recently, KMD analysis was extended to polymer research (19) by using the exact mass of the relevant repeat unit as the reference mass to calculate defects and further developed with the use of fractional base units (20). This has allowed the visualization of complex mass spectra in resolution-enhanced KMD plots (21). The use of mass defect analysis has been also used in metabolomics (22) and mass remainder analysis (MARA) for an elemental compositional assignment algorithm (23).

2.2. Categorization

Elemental compositions are commonly assigned using the form $\text{C}_c\text{H}_h\text{N}_n\text{O}_o\text{S}_s$, where c , h , n , o and s are the numbers of the respective elements. The compositions are then categorized according to (a) heteroatom class, (b) DBE, and (c) carbon number. For instance, species corresponding to

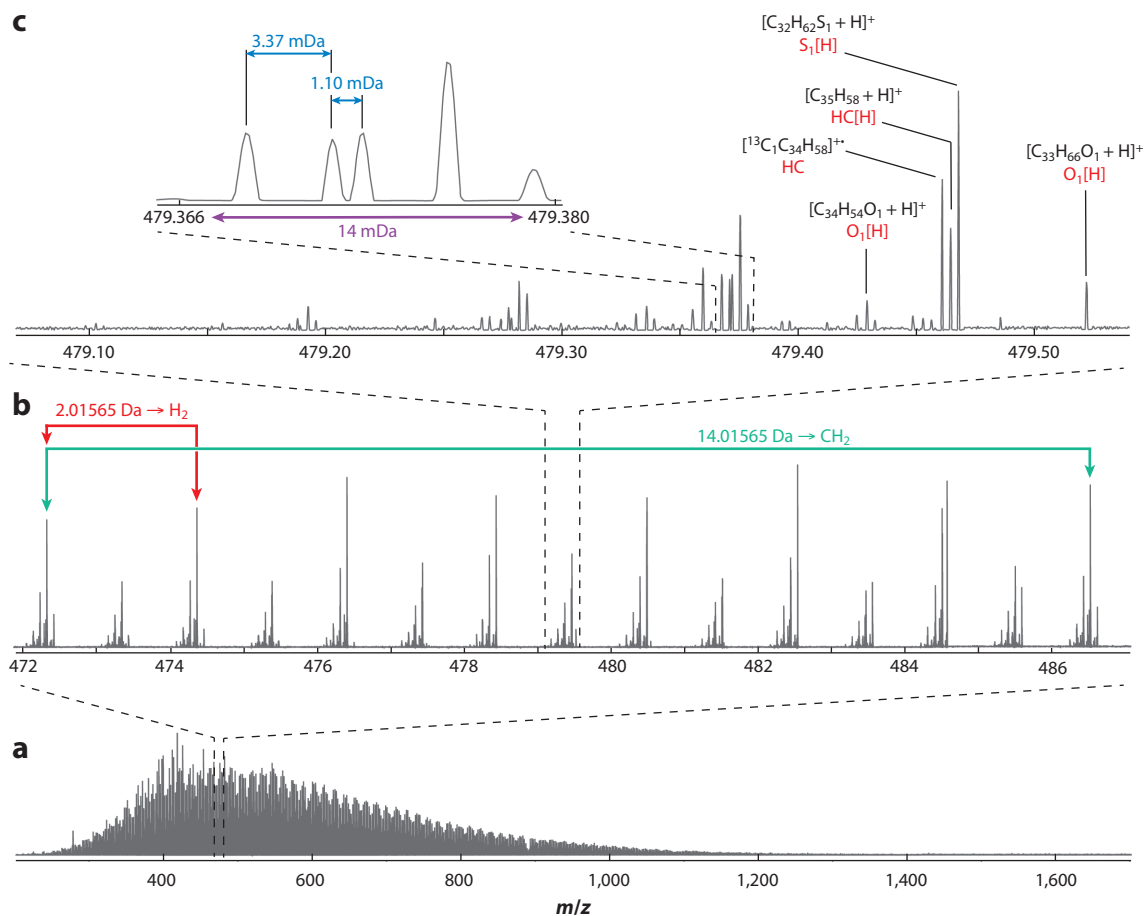


Figure 1

(a) Mass spectrum in absorption mode of a NIST crude oil obtained by positive-ion APPI FTICR MS. (b) Homologous series of species separated by 14.01565 Da and 2.01565 Da, typical of petroleum-related substances. (c) Enlarged region at nominal mass m/z 479, showing selected assignments, class designations, and common mass splits. The mass difference of 3.37 mDa corresponds to C_3 versus H_4S , and the mass difference of 1.1 mDa corresponds to C_4 versus $^{13}C H_3S$. Abbreviations: APPI, atmospheric pressure photoionization; FTICR MS, Fourier transform ion cyclotron resonance mass spectrometry; NIST, National Institute of Standards and Technology.

class HC have general molecular formulae C_cH_h , species including only two sulfur atoms would be designated to class S_2 , and so forth; ion types are also reflected, where the tag [H] is sometimes used to denote protonated or deprotonated species, while an absence of this tag indicates radical ions. The DBE of each composition is calculated using Equation 9:

$$DBE = c - \frac{b}{2} + \frac{n}{2} + 1. \quad 9.$$

Petroleomics data are typically presented in four main plot types: heteroatomic class contribution, DBE versus carbon number (4) (Figure 2), KMD versus nominal Kendrick mass (16, 18), and van Krevelen plots of H/C versus O/C ratios (24, 25). Van Krevelen plots have been extended to three-dimensional (3D) space, with the third dimension used for the relative peak intensity

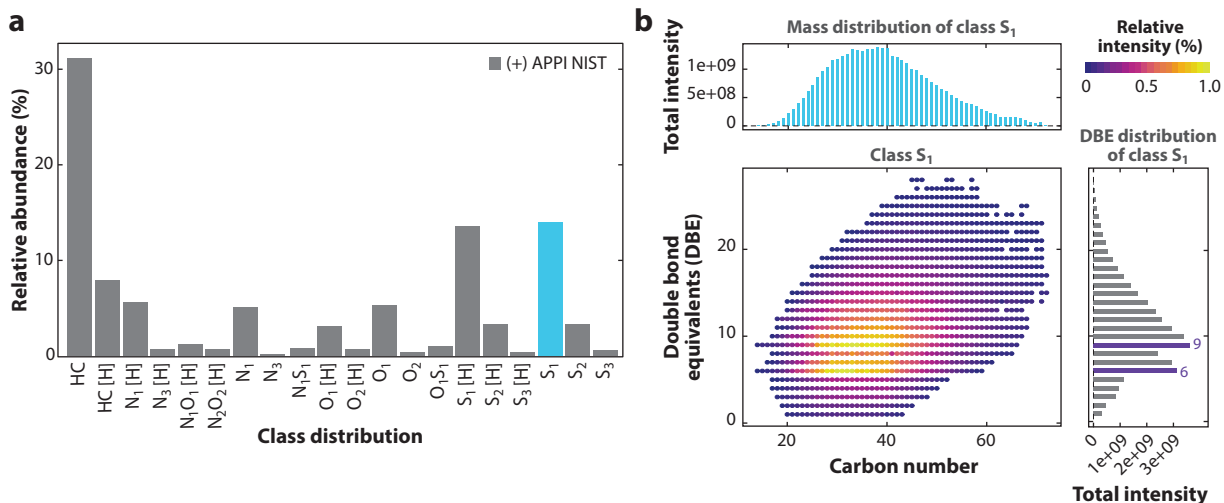


Figure 2

Petroleomics plots obtained using data shown in **Figure 1**. (a) Heteroatom class distribution and (b) double bond equivalent (DBE) versus carbon number for the S₁ class. The projection above the DBE plot shows the carbon number distribution of the S₁ class, while the projection to the right of the DBE versus carbon number plot represents the total intensity contribution at each DBE. Species with a DBE of 6 and 9 are detected at higher relative abundance, a trend commonly observed in the S₁ class.

(26) or an additional ratio axis (27), which allows the H/C, O/C, and N/C ratios to be compared simultaneously.

2.3. Complex Organic Mixtures

Petroleomic tools have been utilized in the analysis of crude oil and their fractions (3, 4, 13), dissolved organic matter (DOM) (28–31), biofuels (32, 33), oil sands (34), bitumen (35, 36), and lignin (37, 38), with a wide range of related studies that include environmental applications. The main complex mixture types may be summarized briefly as follows.

- Crude oils: A mixture of thousands of compounds in which the major elements are carbon (85–95%) and hydrogen (10–14%), followed by sulfur (0.2–3%), nitrogen (<0.1–2%), and oxygen (1–1.5%), plus trace organometallic compounds. Crudes can be separated into four fractions: saturates, aromatics, resins, and asphaltenes (SARA), depending on their solubility and polarity (39). Extra-heavy crude oils, with specific gravity lower than the density of water (or less than 10° American Petroleum Institute gravity) (40), are one of the largest reserves of oil and can contain 40–60% vacuum residue (a fraction with boiling point >540 °C or 540+ atmospheric equivalent temperature) (41).
- Bio-oils: A sustainable source of energy, biomass-derived fuels can be generated from lignocellulosic materials (42). The fuel produced is a complex mixture of oxygenated and nonoxygenated hydrocarbons. Its properties include low calorific value, high oxygen and water contents, low pH, low stability, and immiscibility with conventional petroleum (32).
- Natural organic matter (NOM) and DOM: Products of plant and animal tissue decay that may be found in soil, sediments, and natural water, or as aerosol in the atmosphere (43, 44). NOM consists largely of carbon, hydrogen, and oxygen, and contributions from

heteroatoms such as nitrogen, sulfur, and phosphorus are found in minor traces (12). DOM may be defined as the components capable of passing through a 0.45- μm filter pore (43). DOM is predominantly found in oceans but may also be detected in terrestrial sources such as biomass, soil, and plant litter before being transferred to waterways. Assessing the composition of NOM and DOM is a pivotal environmental and ecological concern and can aid the understanding of global carbon and other elemental cycles (43).

- Oil sands: A natural mixture of clay, sand, water, and bitumen. Bitumen is highly viscous and immobile in reservoir conditions (45, 46). The production of synthetic oil engenders a high cost and considerable impact on the environment; 2–4 barrels of water are required to produce 1 barrel of oil (47), with the water subsequently stored in expansive on-site tailings ponds (48). One of the major areas of environmental concern is therefore oil sands process-affected water (OSPW), a complex mixture that includes polycyclic aromatic hydrocarbons (PAHs), naphthenic acids (NAs) known to be toxic to aquatic organisms, and trace elements (e.g., metals and metalloids). Short- and long-term sustainable water management practices, such as recycling and remediation, are required while minimizing the effects on human health and the natural environment.

3. ANALYTICAL CHALLENGES

The primary analytical challenges for complex mixture characterization can be summarized as follows:

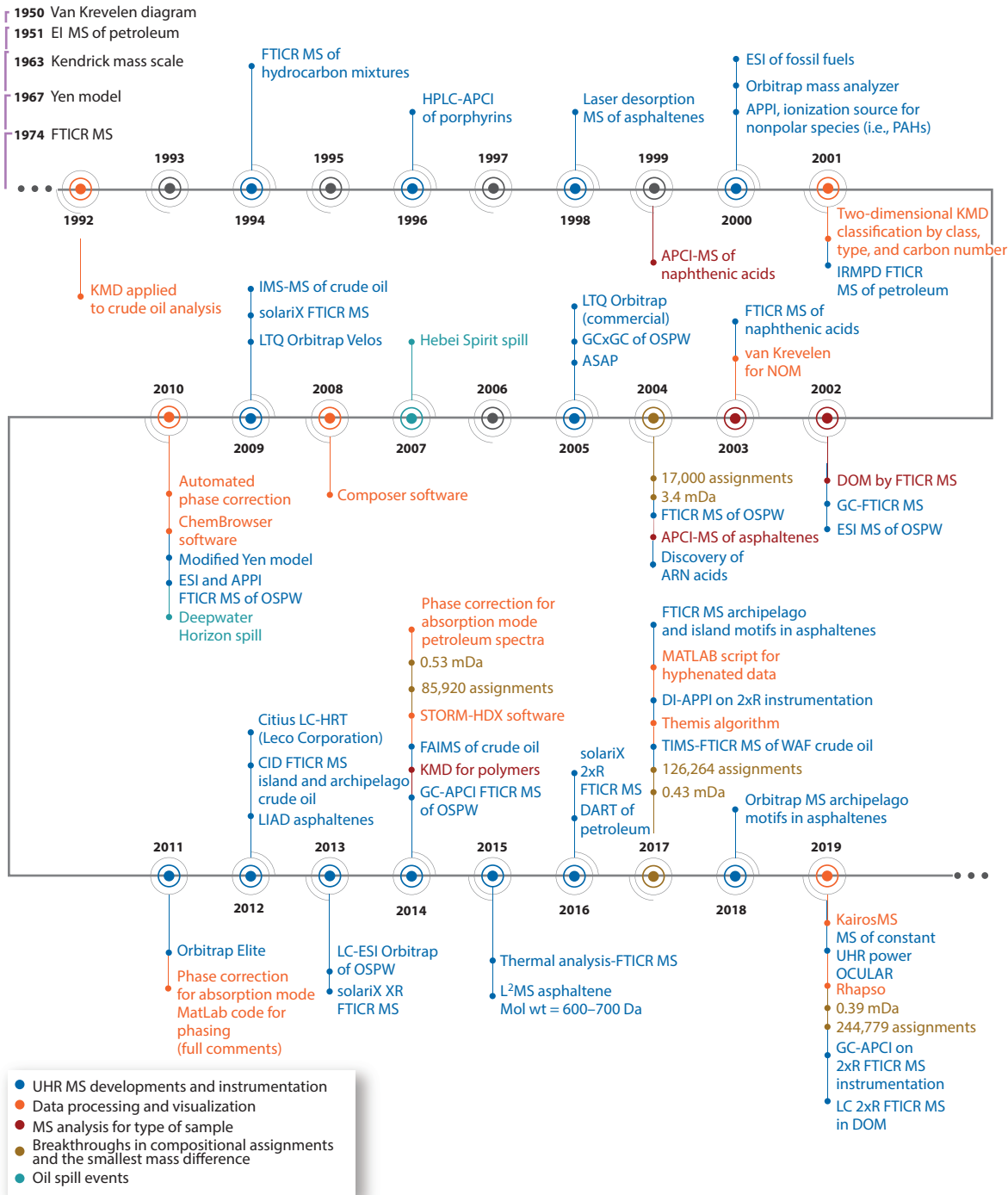
- Ionization: As a consequence of chemical complexity, comprehensive characterization requires the use of a combination of ionization methods.
- Resolving power and mass accuracy: Unique assignments can only be attained if compositions with very small mass difference can be separated from one another.
- Isomer separation: MS coupled to prior separation is required to differentiate structural isomers of species with the same elemental composition.
- Data handling and visualization: The growing size and complexity of the data necessitate that software and new visualization tools need to be developed.

A time line summarizing selected advances in the field of petroleomics is shown in **Figure 3**.

3.1. Ionization

A variety of ionization sources have been used for the study of petroleum (49) and petroleum-related substances (50); two of the most commonly used are ESI and APPI. In ESI, a solution is passed through a capillary, at a high voltage, forming charged droplets. The solvent component of the droplet evaporates, concentrating the charge; once the charge exceeds the Rayleigh limit, the droplet dissociates generating charged ions. ESI generally ionizes more polar components: basic polar species in positive (+) mode and acidic polar species in negative (–) mode. In APPI the sample solution is vaporized and then absorbs photons emitted by a discharge lamp, forming ions. APPI ionizes a wider range of compounds than ESI (49), including nonpolar compounds.

Other atmospheric pressure ionization methods have been used to perform petroleomics analyses, including atmospheric pressure laser ionization (APLI) (51–53). In APLI, radical species predominate, and the technique ionizes a broader range of compounds than ESI, with sensitivity toward nonpolar aromatic hydrocarbons (52). In atmospheric pressure chemical ionization (APCI), the compounds are ionized by a corona discharge needle after desolvation. APCI has been



(Caption appears on following page)

Figure 3 (Figure appears on preceding page)

Summary of the main developments in UHR MS instrumentation, data processing, and visualization. A summary of the total individual elemental compositions, the smallest mass splits, and oil spill events are also reported. The developments of UHR MS instrumentation and data analysis have been of pivotal importance for the development of new fields, the analysis of more complex samples, and further insights into the isomeric composition of complex mixtures. From 17,000 compositions in a crude oil reported in 2004 to almost a quarter of a million compositions reported in 2019, crude oils have proved to be the most complex natural organic composition, challenging FTICR MS capabilities and promoting new analytical methods and software developments. References for this figure can be found in the **Supplemental Materials**. Abbreviations: APCI, atmospheric pressure chemical ionization; APPI, atmospheric pressure photoionization; ARN, high molecular weight naphthenic acids; ASAP, atmospheric solids analysis probe; CID, collision-induced dissociation; DART, direct analysis in real time; DI, direct infusion; DOM, dissolved organic matter; EI, electron ionization; ESI, electrospray ionization; FAIMS, high field asymmetric waveform ion mobility spectrometry; FTICR MS, Fourier transform ion cyclotron resonance mass spectrometry; GC, gas chromatography; GCxGC, two-dimensional GC; HPLC, high-performance liquid chromatography; IMS, ion mobility spectrometry; IRMPD, infrared multiphoton dissociation; KMD, Kendrick mass defect; LC, liquid chromatography; LIAD, laser-induced acoustic desorption; mol wt, mean molecular weight; NOM, natural organic matter; OCULAR, operation at constant ultrahigh resolution; OSPW, oil sands process-affected water; PAH, polycyclic aromatic hydrocarbon; UHR MS, ultrahigh resolution mass spectrometry; WAF, water accommodated fraction.

Supplemental Material >

commonly used when coupling GC (54, 55), and APCI generally ionizes less-polar and smaller molecules than ESI (12).

Hertzog et al. (50) used a combination of ESI, APPI, and laser desorption ionization (LDI) methods for the analysis of bio-oils. ESI, APPI, and LDI were found to ionize more highly saturated compounds, more unsaturated compounds, and compounds with intermediate saturation, respectively. Although LDI can ionize a wide range of crude oil species, it is well known that high laser fluence leads to greater fragmentation and accompanying formation of carbon clusters (fullerenes) characterized by 24-Da separations (56, 57).

Laser-induced acoustic desorption (LIAD) utilizes laser pulses fired onto the rear side of a titanium foil, with sample deposited on the other side. The laser pulses generate acoustic waves that vaporize the samples as neutral molecules, which can then be ionized by electron bombardment or chemical ionization (58). The technique may be particularly useful for analyzing samples of lower volatility and has been applied to the analysis of asphaltene molecular weight distributions.

Atmospheric solids analysis probe (ASAP) ionization has been used for analysis of crude oils and paraffins by TOF MS (59, 60). ASAP provides a rapid analysis without any sample preparation, as the sample can be applied directly to the glass capillary probe of the source. The ionization mechanism in ASAP is analogous to APCI with both protonated and radical ions formed.

In addition to the ionization method selected, the ionization polarity used in an experiment determines the ions observed. Additionally, ion suppression and matrix effects can change the ionization profile of a sample. Peru et al. (40) showed that solvent pH has a significant impact on the class distribution of naphthenic acid fraction compounds detected by (–) ESI MS. In a series of chromatographic separations used to assess ionization selectivity, Rodgers et al. (61) demonstrated that a range of ionization methods preferentially ionize the lower molecular weight species (62).

3.2. Resolving Power and Mass Accuracy

The resolving power and mass accuracy are defining performance characteristics of UHR mass spectrometers. As instrumentation continues to advance and capabilities increase, ever-greater compositional understanding of complex mixtures is afforded.

3.2.1. UHR MS developments. The mass accuracy and resolving power of FTICR mass spectrometers can be increased by increasing the strength of the superconducting magnet. In early 2018, the first two 21 tesla (T) instruments to be brought into operation were applied to the

analysis of complex mixtures. The literature demonstrated a resolving power of 2,700,000 at m/z 400 with a 6.3-s-length transient and absorption mode (63), and a resolving power of 1,200,000 at m/z 393 with a 3-s transient and magnitude mode (64).

An alternative approach to increase resolving power was presented by Nikolaev and coworkers in 2012 (65). The new dynamically harmonized ICR cell design (ParaCell) compensates for inhomogeneities, extending the detection time and, in consequence, increasing the resolving power. The ParaCell is currently implemented in Bruker Daltonics' solariX XR, solariX 2xR, and scimaX, and in the 21 T FTICR mass spectrometer located at the National High Magnetic Field Laboratory (65, 66). FTICR mass spectrometers can now operate using quadrupolar (2ω) detection; while conventionally two electrodes are used for detection, quadrupolar detection utilizes four electrodes. Instrumentation equipped with 2ω detection can therefore offer double resolution for a set acquisition time or equivalent resolution in half the time, making it particularly well suited to hyphenation with chromatographic methods. Cho et al. (67) demonstrated the use of a 7 T FTICR equipped with 2ω detection for the analysis of crude oil, achieving a mass resolving power of 1,500,000 at m/z 400. The 7 T FTICR instrumentation equipped with 2ω detection was also used for hyphenated GC experiments by Thomas et al. (55) for profiling of environmental contaminants in soil core samples from Staten Island, and for hyphenated LC experiments by Kim et al. (68) for the analysis of NOM.

Orbitrap instruments continue to advance, with the recent development of the MegaOrbitrap analyzer achieving favorable performance comparable to a 7.2 T FTICR instrument (69) for the analysis of petroleum samples. Specifically, a resolving power (in absorption mode) of 841,000 at m/z 400 was an improvement of more than twofold when compared to the resolving power of 337,100 achieved on the 7.2 T FTICR instrument.

A summary of resolving powers achieved by UHR mass spectrometers for the analysis of complex mixtures can be found in **Table 1**.

3.2.2. Absorption mode. Phase correction is a data processing method that increases the resolving power of Fourier transform MS instruments by up to a factor of two and improves the signal-to-noise by a factor of $\sqrt{2}$ compared to traditional magnitude mode (8). Absorption mode is available for both FTICR and Orbitrap instruments.

3.2.3. Spectral stitching. Spectral stitching is a growing area of interest for FTICR and Orbitrap MS, allowing space-charge effects to be reduced and leading to an increase in resolving power. Stitching employs a mass filter, such as a quadrupole, to selectively accumulate ions for a succession of narrow m/z windows. The resulting mass spectra are then stitched together to generate a mass spectrum spanning the entire m/z range. Gaspar & Schrader (70) demonstrated a sevenfold increase in the number of assigned peaks when using a spectral stitching approach with FTICR MS. Vetere & Schrader (71) showed that spectral stitching can be used with Orbitrap mass analyzers to improve sensitivity, yielding an up to tenfold increase in the number of assignments compared to a nonstitched experiment. In 2017 Krajewski et al. (72) achieved 126,264 assignments using an 8-s acquisition for each mass window. While this approach reduced space charge and extended the mass range detected, the typical drop in resolving power with increasing m/z was not overcome, and higher m/z species were therefore not resolvable.

3.2.4. OCULAR. Palacio Lozano et al. (13) recently developed a new method named operation at constant ultrahigh resolution (OCULAR). OCULAR uses narrow m/z segments of increasing acquisition times by raising the low m/z cutoff of each subsequent window, maintaining a near constant resolving power across the full mass range. Additionally, a novel algorithm, named Rhapsody,

Table 1 List of resolving powers obtained by UHR MS analysis of complex organic mixtures, reported in the literature since 2012^a

Year	Instrument type	Sample type	Resolving power	Acquisition time (s)	Notes	Reference
2012	12 T LTQ	Petroleum	380,000 (<i>m/z</i> 400)	1.4	12,573 assignments, stitched data	70
2016	21 T homebuilt	Organic matter	1,200,000 (<i>m/z</i> 367)	3	Magnitude mode, SD of 0.09 ppm	64
2017	9.4 T homebuilt	Petroleum	1,700,000 (<i>m/z</i> 400)	8	126,264 assignments, stitched data, absorption mode, RMS error of 0.13 ppm	72
2017	Orbitrap	Petroleum	960,000 (<i>m/z</i> 400)	3	71,166 assignments, stitched data, absorption mode, sub-ppm mass errors	71
2018	MegaOrbitrap (modified Orbitrap Elite)	Petroleum	841,000 (<i>m/z</i> 400)	3	Absorption mode, mass error of 0.93 ppm	69
2018	21 T homebuilt	Organic matter	2,700,000 (<i>m/z</i> 400)	6.3	49,040 assignments, absorption mode, mass error of <0.5 ppm	63
2019	7 T solariX 2xR	Petroleum	300,000 (<i>m/z</i> 400)	1.5	Average mass error of 0.29 ppm	73
2019	12 T solariX	Petroleum	1,792,000 (average for <i>m/z</i> 270–1,000)	2.3 to 10.7	50,000 assignments, constant resolving power across the full <i>m/z</i> range, absorption mode, OCULAR method	13
2019	12 T solariX	Petroleum	3,120,000 (average for <i>m/z</i> 260–1,505)	5.4 to 32	244,779 assignments, constant resolving power across the full <i>m/z</i> range, absorption mode, RMS mass error of 0.11 ppm, OCULAR method	13

^aFor the measured resolving power, the associated *m/z* is listed in each case.

Abbreviations: OCULAR, operation at constant ultrahigh resolution; RMS, root mean square; SD, standard deviation.

was developed to facilitate noise removal, correct signal attenuation, and perform the segment stitching. OCULAR enabled analysis of an extremely challenging truly nondistillable fraction of crude oil, with a record number of 244,779 unique molecular assignments at a near constant resolving power of approximately 3 million. The method reduces space-charge effects and increases resolving power, mass accuracy, and dynamic range, and can be used across multiple instrument designs, improving both low- and high-field instrument performance.

3.3. Isomer Separation

Various chromatographic methods have been coupled to UHR MS, utilizing separation to reduce matrix effects and identify previously low ion yield species, and with the aim of structural feature identification through isomer resolution. Online chromatography, where the eluent from the column is directly transferred to the mass spectrometer, offers isomeric information through the

generation of extracted ion chromatograms (EICs) of individual molecular compositions. The data analysis and processing time is greatly increased when compared to direct infusion data, however, given that each experiment represents approximately 1,000 MS scans (74). Offline separation, or fractionation, has also been widely used, imparting greatly reduced time resolution but offering the advantage of simplified data analysis.

GC was first coupled to FTICR instrumentation in 1980 (75) and used for the fingerprinting of complex fuel samples in 2002 (76). GC separates components largely by boiling point, but only volatile species can be accessed, which limits the applicability of GC to light and medium cuts of crude oils. GC-APCI-FTICR MS has been used for the analysis of OSPW (54), fuels and particulates (77, 78), and environmental samples (55). Additionally, GC-APLI-FTICR MS and GC-APPI-Orbitrap MS have been applied to the analysis of crude oils (53, 79). LC has been used for NOM characterization by LC-ESI-FTICR MS (68), while high-performance liquid chromatography (HPLC)-ESI-Orbitrap MS with a size exclusion column has been used for the study of DOM (80). LC suffers greater band broadening than GC, which leads to lower resolution of isomers, although the technique is more useful for lower boiling point samples. The need for LC-compatible solvents can preclude those commonly used for petroleum analysis, such as toluene, which in turn restricts the ionization sources that can be coupled with LC. SFC allows elution of high-molecular-weight components inaccessible by GC and has been successfully coupled with APCI-Orbitrap MS for the analysis of isomeric compositions of OSPW (81).

TIMS is a development of ion mobility spectrometry, in which ions are initially trapped using radially confining radiofrequency voltages and an axial electric field that counteracts the drag force from the flow of gas. Ions are eluted as the magnitude of the axial field is progressively increased (82). Ion mobility techniques coupled with mass spectrometers are used to separate isomers and ions according to their collision cross section (which, in turn, allows the size or shape of the structure to be elucidated), charge, and drift gas polarizability (83, 84). TIMS coupled to FTICR MS has been used with several complex mixtures, including PAHs (85), NOM (86), DOM (87), and aerosols (88).

A variety of offline fractionation and separation methods, in addition to traditional SARA separation, may be used to address selective ionization (61). Thin-layer chromatography coupled with LDI has also been assessed for use with crude oil fractions (89).

3.4. Data Handling and Visualization

The need to more efficiently analyze data, visualize samples, enable fingerprinting, and improve comparisons between samples continues to grow. Several new types of visualizations have been recently developed.

One development is aromaticity index (AI), developed by Koch & Dittmar (90, 91). The AI reflects the C-C double bond density in a given molecule and is a parameter that can be calculated solely from the exact masses of single NOM compounds. A modified AI parameter termed AI_{mod} can be calculated by assuming that only half the oxygen is present in carbonyl groups; however, this procedure requires additional bulk sample information. AI_{mod} values of ≥ 0.5 may be described as indicators of aromatic compounds (92), values ≥ 0.67 are unambiguous indicators of aromatic compounds, and values < 0.5 correspond to nonaromatic compounds (92). The AI parameter is typically used in conjunction with a van Krevelen plot for data visualization, with different AI values mapped to data point color (93).

Zhuov et al. (94) developed a hexagonal class representation for characterization of an entire sample. Using 3D vector space, each axis represents a commonly found heteroatom: N, O, and S. Each heteroatom class can then be represented by its (N, O, S) coordinate. This type of

representation facilitates sample comparison and may be applicable to fingerprinting, having been applied to both fuels (77) and crude oil (72).

3.4.1. Interactive visualization software. The growth of data processing technologies, such as Python and R programming languages, as well as associated data manipulation and plotting, have enabled researchers to develop interactive analysis and visualization tools. Bioconductor, a toolbox of curated R packages, has been widely used to great effect within the metabolomics and proteomics communities (95) to produce software-enhanced analysis. Only recently, however, has development of visualization tools for petroleomics started to grow (95).

Kew et al. (96) published their *i*-van Krevelen tool, which was developed in Python to generate interactive visualizations that can then be accessed through an internet browser. The tool incorporates a centroid mass spectrum, van Krevelen diagram, DBE versus carbon number plot, and modified AI versus carbon number plots. A key feature is the linking of several interactive plots, so that data selected in one plot highlight the same points in other plots, enabling rapid comparison across several differing plot types.

Another browser-based tool is UltraMassExplorer (97), offering a complete data evaluation process, from assignment of elemental compositions to data visualization. UltraMassExplorer was written in the R language and utilizes the Shiny package to generate the Web application. Compositional assignments are performed using a library-based approach built upon the rules suggested by Kind & Fiehn (98). The interactive visualizations include 2D and 3D van Krevelen plots, with the 3D plot allowing free rotation and enlargement of data set regions.

3.4.2. Statistical methods. Statistical treatments of data following complex mixture analysis are becoming commonplace; multivariate analyses perform well in translating raw data into a model (99). Approaches such as principal component analysis (PCA) have previously been applied to petroleomics samples to indicate variability between samples (100, 101). Similarly, Hur et al. (102) have recently applied the volcano plot, a scatterplot of univariate analysis, to the analysis of petroleomics data. The volcano plots were generated by plotting statistical significance (*p*-value) versus degree of change (fold change), where fold change is positive if the peak magnitude is higher in the second sample than in the first. The plots can then be used for characterization or as a filter by only selecting significant peaks. The filtered peaks are then plotted using traditional DBE versus carbon number plots and van Krevelen plots.

Another area of statistical analysis has been the treatment of replicate data sets. In 2017, Gavard et al. (103) developed the Themis algorithm for batch processing of replicate data sets. The Themis algorithm utilizes several steps to ensure reproducibility: detection of anomalous replicates, normalization of peak magnitudes, alignment of peaks across replicates, and removal of inconsistent peaks to produce a combined peak list.

4. EXAMPLES OF APPLICATIONS

4.1. Crude Oil

Only the lowest boiling or polar components (104) and average or bulk properties (105, 106) of crude oils can be assessed using conventional analytical techniques (107). Studies of crude oils using UHR MS methods include characterization of whole oils (69) and SARA fractions following prior separation (108–110). Extensive studies of multiple petroleum samples have demonstrated that the profiles obtained using FTICR MS correlate with bulk properties (110). The analysis of crude oils has also included focused investigation into the naphthenic acids (111, 112) and

sulfur-containing (113–115) compounds known to cause corrosion in refineries (116, 117). In addition to causing corrosion, sulfur-containing compounds are prone to fouling catalysts used to hydrotreat sour crude oils (116), and removal of sulfur can be particularly problematic when contained within thiophenic structures (118, 119). Recent work has focused on the analysis of polar sulfur compounds and sulfoxides in crude oils, which could lead to developments in catalysts and improvements in desulfurization processes (113). Fragmentation of different crude oil cuts has demonstrated that sulfur is located in a diverse range of structures and may be more difficult to remove in heavier fractions (114).

4.2. Asphaltenes

Asphaltenes are defined as the fraction of crude oil insoluble in *n*-alkanes, such as *n*-heptane, and soluble in aromatic solvents, such as toluene. Asphaltenes are known for causing major problems in downstream and upstream processing (120) due to their propensity to flocculate above a critical concentration (120), under extreme conditions (121), or when constituent in an incompatible blend (122), and their subsequent deposition is a major problem in the field. Asphaltenes consist of PAH cores (123), may contain heteroatoms such as N, O, or S, and exist as island or archipelago structures, defined as a single alkyl-substituted PAH core or multiple PAH cores bridged by alkyl chains, respectively (124, 125). Fragmentation methods such as collision-induced dissociation (CID) (126), high-energy collision dissociation (HCD) (127), and infrared multiphoton dissociation (IRMPD) have been used to assess the prevalence of island and archipelago asphaltenes in different petroleum samples (128).

4.3. Environment

Assessing the impact of petroleum on the environment is an important application of petroleomics (55, 129). The long-term effects of anthropogenic activities, including major spills into the New York/New Jersey Estuary, were assessed by studying the hydrophobic components of soil sampled at a range of depths (55). Following the Hebei Spirit spill in South Korea, FTICR MS was used for fingerprinting and demonstrated that there had been a significant increase in polar species containing N, O, and S in weathered oil (129). In the aftermath of the Deepwater Horizon incident (130) in the Gulf of Mexico, GC studies demonstrated that hydrocarbon residues from multiple contamination sites exhibited increasing O content over 18 months (131), whereas studies employing FTICR MS showed that Macondo well oil irradiated with simulated sunlight has a greater proportion of O₅- and N₁O_x-containing compounds concurrent with a decrease in O₂ and N₁ compounds relative to a dark control sample (132). In an earlier FTICR MS study published in 2014, Griffiths et al. (133) investigated the effects of simulated sunlight on crude oil, with respect to heteroatom class and DBE. In a study demonstrating the persistence of petroleum contaminants, contributions from the HC class decreased over time and were not detected 43 months after the Deepwater Horizon spill, concurrent with an increase in oxygen-containing compounds, in samples extracted from salt marsh sediments (134).

4.4. Oil Sands

High-resolution LC-MS and GC × GC-MS have recently been used to study oil field-produced water, tentatively identifying constituents and assessing the importance of these unknowns as potential toxicity contributors (135). Similarly, monitoring the impact of oil production on the environment by analyzing OSPW presents another important petroleomics application (136).

Petroleomics methodologies are regularly used to understand OSPW composition (136–138) and toxicity as it ages (139, 140). Recent research has demonstrated the effectiveness of catalytic processes aimed at reducing the concentration of organic compounds in OSPW, a promising prospect for the remediation of tailings ponds sites (34). The impact of experimental parameters on the observed OSPW profile has also been demonstrated, which may lead to the development of more robust environmental monitoring (40, 47).

4.5. Biofuels

With production shifting to unconventional oil sources, petroleomics methodologies also play a role in profiling renewable fuels, such as bio-oils (32, 141). As oxygen-containing species predominate in bio-oils, van Krevelen (24) plots are used widely for their analysis (142), with the population density at coordinate locations known to be characteristic of differing biogeochemical compound classes such as lignin, fatty acids, and carbohydrates (26, 142, 143). Although desorption APPI allowed biochar to be studied without the need for sample dissolution (144), the use of complementary ESI, APPI, and LDI allowed the composition of biochars produced under different pyrolysis conditions to be compared (33).

4.6. Natural Organic Matter/Dissolved Organic Matter

Advancing petroleomics methodologies and capabilities benefit other research fields, such as the study of NOM (145) and DOM (63, 146), and including the use of H/D exchange reactions to characterize oxygen functionalities (145). Fingerprinting of DOM from spatially distinct surface waters has allowed the identification of common and unique formulae and aided understanding of observed differences between their reactivity in aquatic processes (29). More recently, FTICR MS has been used in combination with other analytical methods to compare the profiles of DOM and disinfection by-products in untreated and treated ship ballast (31). Hyphenated techniques have also been used in recent studies of DOM, including HPLC-Orbitrap MS/MS (147) and a recent study that used TIMS-FTICR MS to assess the isomeric diversity, with approximately 6–10 isomers per molecular formula assigned (28).

4.7. Compositional Space of Complex Mixtures

The remarkable difference in oxygen-containing species between crude oil and other complex mixtures, such as bio-oils and DOM, defines their distinctive compositional space. For instance, asphaltenes and crude oil in general typically comprise hydrocarbons with up to five N, O, and S heteroatoms; in contrast, the compositional space of DOM comprises species that can contain up to 30 oxygen atoms (12). In **Figure 4**, (–) ESI data for a Suwannee River fulvic acid (SRFA) standard, as an example of a complex NOM-type sample, and (+) APPI data for asphaltenes are compared. **Figure 4** demonstrates that SRFA compositions are found at lower m/z values, and the total number of compositions assigned by nominal mass is comparatively higher in the asphaltene sample compared to the DOM sample. Additionally, the SRFA assignments are shifted to the lower end of each nominal m/z , indicating a greater hydrogen deficiency. In the particular case of highly oxygenated complex mixtures, the hydrogen deficiency may be attributed to the limitations in number of C, O, and H atoms given the mass range of their compositions (26). As can be seen in the van Krevelen diagrams for the two samples, distinctive molecular distributions can be observed. In general, DOM compositions are distributed across the van Krevelen diagram, while asphaltene compositions have predominantly low O/C ratios.

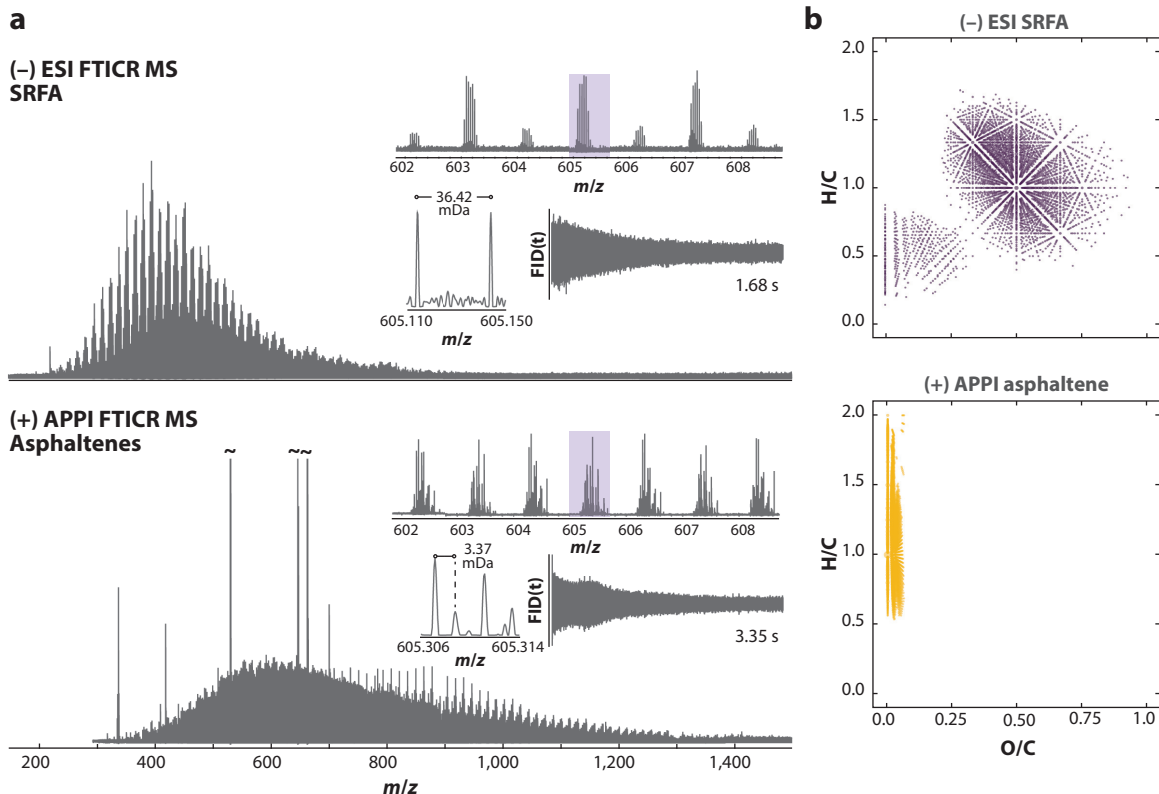


Figure 4

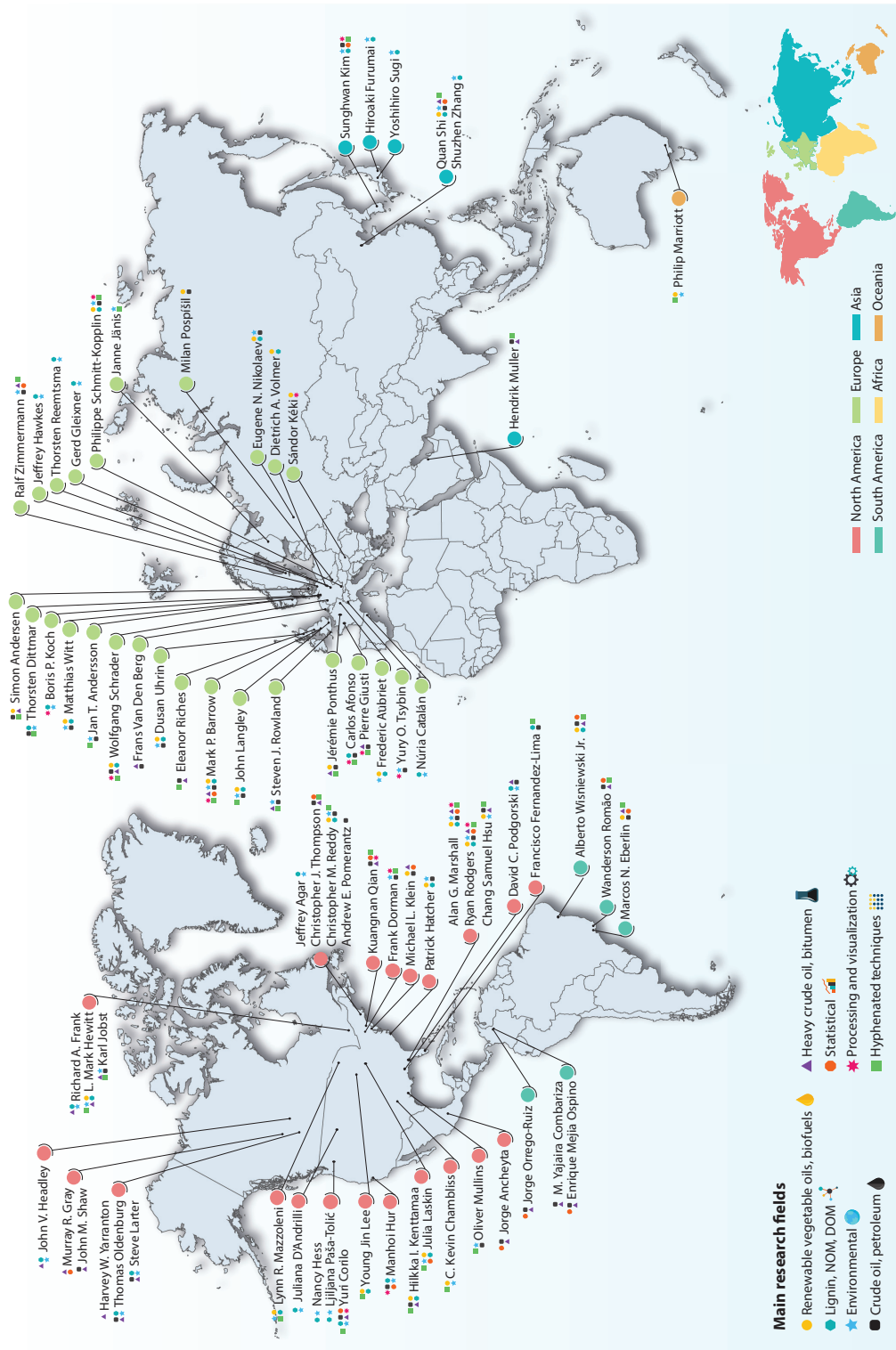
Comparison of the mass distribution of SRFAs obtained by (–) ESI FTICR MS and asphaltenes from a Mexican crude oil obtained by (+) APPI FTICR MS (*a*). Note that the SRFA and asphaltene mass spectra were obtained at 4 M and 8 M, respectively. Therefore, a longer transient and, in turn, a higher resolving power were achieved for the asphaltene sample. In general, species with smaller mass difference are detected in crude oils and their fractions. A mass split of 3.37 mDa corresponding to C₃ versus SH₄ is commonly found in crude oil when using APPI. A total of 40 and 13 individual molecular compositions were assigned at *m/z* 605 in the asphaltene and SRFA mass spectra, respectively. Visualization using van Krevelen plots allows the oxygen-to-carbon ratio (O/C) and hydrogen-to-carbon ratio (H/C) of multiple molecular assignments to be compared simultaneously (*b*). Abbreviations: APPI, atmospheric pressure photoionization; ESI, electrospray ionization; FID, free induction decay; FTICR MS, Fourier transform ion cyclotron resonance mass spectrometry; SRFA, Suwannee River fulvic acid.

5. FUTURE ISSUES

Despite the recent developments in petroleomics and the analysis of other complex mixtures, there remain pertinent and immediate challenges in the field.

Although a plethora of ionization methods are available, offering complementary information by preferentially accessing different compound types, there are undoubtedly fractions of petroleum that currently remain unseen, even with prior separation improving access to the compositional space (109, 148, 149). Where samples are solid or absorbed in situ, for example, asphaltene deposits or biochar, the challenge remains to successfully desorb intact molecules to avoid overcomplicating the resulting spectrum with fragments or adducts and to provide a representative analysis of nonhomogeneous substances (144).

The relative abundance or intensity of compounds detected in MS is known to be dependent on a multitude of factors, including relative ionization efficiencies, concentration, sample preparation



(Caption appears on following page)

Examples of researchers working in petroleomics and related fields. The research groups perform detailed analysis of complex organic mixtures and investigate their properties and reactivity. Categories of different sample types and method developments are shown. Abbreviations: DOM, dissolved organic matter; NOM, natural organic matter.

steps, matrix interferences, ionization parameters, and instrument tuning parameters. The impact of these factors on observed profiles needs to be better understood, particularly when comparing recently acquired and historical data, or data obtained at different laboratories.

Given that the relative abundance of different compounds cannot be taken to relate directly to their concentration, quantification of individual components remains a major challenge for petroleomics. The use of standards spiked at known concentrations for hyphenated experiments may make possible quantification of known compounds of concern, although quantification of a broader range of components, particularly those with high isomeric diversity (147), presents a greater task (104). The use of hyphenated techniques would also allow the isomeric complexity underlying each molecular composition to be better understood.

With the shift toward petroleum production from unconventional sources continuing, the characterization of ever heavier and more complex samples presents an ongoing challenge. While a record resolving power of 3 million across the full mass range (m/z 260–1,505) has recently been achieved, to resolve the mass split of 0.1 mDa at m/z 1,000, a resolving power of around 10 million will be required (13, 104).

While UHR MS is capable of unrivaled compositional analysis of petroleum samples, assessment of molecular structure remains a challenge. Methods including CID and IRMPD fragmentation can be used on small mass windows, but the inherent complexity of petroleum samples means that multiple compositions and their isomers are fragmented simultaneously. Although isolation, for example, using quadrupoles prior to detection efficient enough to isolate a single molecular assignment would be desirable, the multiple composite isomers would lead to complicated fragmentation spectra representative of several parent ions. For instance, for the single molecular composition $C_{14}H_{10}$, as many as 5.3×10^6 isomers are possible. Prior chromatographic separation of isomers, followed by efficient mass isolation, could afford the separation required for fragmentation of single molecular species and aid our understanding of supramolecular interactions that impact bulk properties (69, 148); results have been achieved for highly simplified samples (150).

Improvements in petroleomics methodologies engender larger and ever more complex data sets, particularly when hyphenated with prior chromatographic separation; the handling of such data presents an ongoing challenge (78, 149). Visualizing and comparing multiple ultracomplex data sets and identifying key differences and similarities between them also become increasingly challenging (104). Data processing software and visualization tools are expected to continue to evolve to keep up with these growing requirements.

Improvements in UHR MS instrumentation, separation, data processing, and visualization all benefit other fields, helping to push the frontiers of complex mixture analysis. As shown in **Figure 5**, a large number of scientists around the world are currently working in the fields of petroleomics and related areas, utilizing the wide variety of UHR MS techniques.

DISCLOSURE STATEMENT

M.P.B. is a trustee and elected member of the executive committee of the British Mass Spectrometry Society (BMSS). He has also received grants and industrial funding in the field of petroleomics. The other authors are not aware of any affiliations, memberships, funding, or financial holdings that might be perceived as affecting the objectivity of this review.

LITERATURE CITED

1. Palit S. 2017. Petroleum engineering, petrochemicals, environmental and energy sustainability: a vision for the future. In *Engineering Technology and Industrial Chemistry with Applications*, ed. RK Haghi, F Torrens, pp. 3–24. New York: Taylor & Francis. 1st ed.
2. Marshall AG, Hendrickson CL. 2008. High-resolution mass spectrometers. *Annu. Rev. Anal. Chem.* 1:579–99
3. Hsu CS, Hendrickson CL, Rodgers RP, McKenna AM, Marshall AG. 2011. Petroleomics: advanced molecular probe for petroleum heavy ends. *J. Mass Spectrom.* 46(4):337–43
4. Marshall AG, Rodgers RP. 2008. Petroleomics: chemistry of the underworld. *PNAS* 105:18090–95
5. Marshall AG, Rodgers RP. 2004. Petroleomics: the next grand challenge for chemical analysis. *Acc. Chem. Res.* 37:53–59
6. Marshall AG, Hendrickson CL, Jackson GS. 1998. Fourier transform ion cyclotron resonance mass spectrometry: a primer. *Mass Spectrom. Rev.* 17(1):1–35
7. Hu Q, Noll RJ, Li H, Makarov A, Hardman M, Cooks RG. 2005. The Orbitrap: a new mass spectrometer. *J. Mass Spectrom.* 40(4):430–43
8. Qi Y, O'Connor PB. 2014. Data processing in Fourier transform ion cyclotron resonance mass spectrometry. *Mass Spectrom. Rev.* 33(5):333–52
9. Fenn JB. 2002. *John B. Fenn Nobel Lecture*. Nobel Media AB, Stockholm. <https://www.nobelprize.org/prizes/chemistry/2002/fenn/lecture/>
10. Hardman M, Makarov AA. 2003. Interfacing the orbitrap mass analyzer to an electrospray ion source. *Anal. Chem.* 75(7):1699–1705
11. Denisov E, Damoc E, Lange O, Makarov A. 2012. Orbitrap mass spectrometry with resolving powers above 1,000,000. *Int. J. Mass Spectrom.* 325–327:80–85
12. Hertkorn N, Frommberger M, Witt M, Koch BP, Schmitt-Kopplin P, Perdue EM. 2008. Natural organic matter and the event horizon of mass spectrometry. *Anal. Chem.* 80(23):8908–19
13. Palacio Lozano DC, Gavard R, Arenas-Diaz JP, Thomas MJ, Stranz DD, et al. 2019. Pushing the analytical limits: new insights into complex mixtures using mass spectra segments of constant ultrahigh resolving power. *Chem. Sci.* 10(29):6966–78
14. McKenna AM, Williams JT, Putman JC, Aeppli C, Reddy CM, et al. 2014. Unprecedented ultrahigh resolution FT-ICR mass spectrometry and parts-per-billion mass accuracy enable direct characterization of nickel and vanadyl porphyrins in petroleum from natural seeps. *Energy Fuels* 28(4):2454–64
15. Kim S, Rodgers RP, Marshall AG. 2006. Truly “exact” mass: elemental composition can be determined uniquely from molecular mass measurement at ~ 0.1 mDa accuracy for molecules up to ~ 500 Da. *Int. J. Mass Spectrom.* 251(2–3):260–65
16. Kendrick E. 1963. A mass scale based on $\text{CH}_2 = 14.0000$ for high resolution mass spectrometry of organic compounds. *Anal. Chem.* 35(13):2146–54
17. Rodgers RP, Marshall AG. 2007. Petroleomics: advanced characterization of petroleum-derived materials by Fourier transform ion cyclotron resonance mass spectrometry (FT-ICR MS). In *Asphaltenes, Heavy Oils, and Petroleomics*, ed. OC Mullins, EY Sheu, A Hammami, AG Marshall, pp. 63–93. New York: Springer
18. Hughey CA, Hendrickson CL, Rodgers RP, Marshall AG, Qian K. 2001. Kendrick mass defect spectrum: a compact visual analysis for ultrahigh-resolution broadband mass spectra. *Anal. Chem.* 73(19):4676–81
19. Sato H, Nakamura S, Teramoto K, Sato T. 2014. Structural characterization of polymers by MALDI spiral-TOF mass spectrometry combined with Kendrick mass defect analysis. *J. Am. Soc. Mass Spectrom.* 25(8):1346–55
20. Fouquet T, Sato H. 2017. Improving the resolution of Kendrick mass defect analysis for polymer ions with fractional base units. *Mass Spectrom.* 6(1):A0055
21. Zheng Q, Morimoto M, Sato H, Fouquet T. 2019. Resolution-enhanced Kendrick mass defect plots for the data processing of mass spectra from wood and coal hydrothermal extracts. *Fuel* 235:944–53
22. Smirnov KS, Forcisi S, Moritz F, Lucio M, Schmitt-Kopplin P. 2019. Mass difference maps and their application for the recalibration of mass spectrometric data in nontargeted metabolomics. *Anal. Chem.* 91(5):3350–58

23. Nagy T, Kuki Á, Nagy M, Zsuga M, Kéki S. 2019. Mass-Remainder Analysis (MARA): an improved method for elemental composition assignment in petroleomics. *Anal. Chem.* 91:6479–86
24. Van Krevelen DW. 1950. Graphical-statistical method for the study of structure and reaction processes of coal. *Fuel* 29:269–84
25. Van Krevelen DW. 1984. Organic geochemistry—old and new. *Org. Geochem.* 6:1–10
26. Kim S, Kramer RW, Hatcher PG. 2003. Graphical method for analysis of ultrahigh-resolution broadband mass spectra of natural organic matter, the Van Krevelen diagram. *Anal. Chem.* 75(20):5336–44
27. Wu Z, Rodgers RP, Marshall AG. 2004. Two- and three-dimensional van Krevelen diagrams: a graphical analysis complementary to the Kendrick mass plot for sorting elemental compositions of complex organic mixtures based on ultrahigh-resolution broadband Fourier transform ion cyclotron resonance. *Anal. Chem.* 76(9):2511–16
28. Leyva D, Tose LV, Porter J, Wolff J, Jaffé R, Fernandez-Lima F. 2019. Understanding the structural complexity of dissolved organic matter: isomeric diversity. *Faraday Discuss.* 218:431–40
29. Niu XZ, Harir M, Schmitt-Kopplin P, Croué JP. 2018. Characterisation of dissolved organic matter using Fourier-transform ion cyclotron resonance mass spectrometry: type-specific unique signatures and implications for reactivity. *Sci. Total Environ.* 644:68–76
30. Zito P, Podgorski DC, Johnson J, Chen H, Rodgers RP, et al. 2019. Molecular-level composition and acute toxicity of photosolubilized petrogenic carbon. *Environ. Sci. Technol.* 53(14):8235–43
31. Ziegler G, Gonsior M, Fisher DJ, Schmitt-Kopplin P, Tamburri MN. 2019. Formation of brominated organic compounds and molecular transformations in dissolved organic matter (DOM) after ballast water treatment with sodium dichloroisocyanurate dihydrate (DICD). *Environ. Sci. Technol.* 53:8006–16
32. Staš M, Chudoba J, Kubicka D, Blazek J, Pospíšil M. 2017. Petroleomic characterization of pyrolysis bio-oils: a review. *Energy Fuels* 31(10):10283–99
33. Cole DP, Smith EA, Lee YJ. 2012. High-resolution mass spectrometric characterization of molecules on biochar from pyrolysis and gasification of switchgrass. *Energy Fuels* 26(6):3803–9
34. Leshuk T, Peru KM, de Oliveira Livera D, Tripp A, Bardo P, et al. 2018. Petroleomic analysis of the treatment of naphthenic organics in oil sands process-affected water with buoyant photocatalysts. *Water Res.* 141:297–306
35. Kostyukevich Y, Solovyov S, Kononikhin A, Popov I, Nikolaev E. 2016. The investigation of the bitumen from ancient Greek amphora using FT ICR MS, H/D exchange and novel spectrum reduction approach. *J. Mass Spectrom.* 51:430–36
36. Smith DF, Rahimi P, Teclerian A, Rodgers RP, Marshall AG. 2008. Characterization of Athabasca bitumen heavy vacuum gas oil distillation cuts by negative/positive electrospray ionization and automated liquid injection field desorption ionization Fourier transform ion cyclotron resonance mass spectrometry. *Energy Fuels* 22(11):3118–25
37. Qi Y, Hempelmann R, Volmer DA. 2016. Shedding light on the structures of lignin compounds: photo-oxidation under artificial UV light and characterization by high resolution mass spectrometry. *Anal. Bioanal. Chem.* 408(28):8203–10
38. Echavarri-Bravo V, Tinzl M, Kew W, Cruickshank F, Logan Mackay C, et al. 2019. High resolution Fourier transform ion cyclotron resonance mass spectrometry (FT-ICR MS) for the characterisation of enzymatic processing of commercial lignin. *N. Biotechnol.* 52:1–8
39. Jewell DM, Weber JH, Bunger JW, Plancher H, Latham DR. 1972. Ion-exchange, coordination, and adsorption chromatographic separation of heavy-end petroleum distillates. *Anal. Chem.* 44(8):1391–95
40. Peru KM, Thomas MJ, Palacio Lozano DC, McMartin DW, Headley JV, Barrow MP. 2019. Characterization of oil sands naphthenic acids by negative-ion electrospray ionization mass spectrometry: influence of acidic versus basic transfer solvent. *Chemosphere* 222:1017–24
41. Behrenbruch P, Dedigama T. 2007. Classification and characterisation of crude oils based on distillation properties. *J. Pet. Sci. Eng.* 57(1–2):166–80
42. Abdelnur PV, Vaz BG, Rocha JD, de Almeida MBB, Teixeira MAG, Pereira RCL. 2013. Characterization of bio-oils from different pyrolysis process steps and biomass using high-resolution mass spectrometry. *Energy Fuels* 27(11):6646–54

43. Nebbioso A, Piccolo A. 2013. Molecular characterization of dissolved organic matter (DOM): a critical review. *Anal. Bioanal. Chem.* 405(1):109–24
44. Reemtsma T. 2009. Determination of molecular formulas of natural organic matter molecules by (ultra-) high-resolution mass spectrometry. Status and needs. *J. Chromatogr. A* 1216(18):3687–701
45. Total. 2004. *Extra-heavy oils and bitumen: reserves for the future*. Rep. INIS-FR-6377, Total S.A., Courbevoie, France. https://inis.iaea.org/search/search.aspx?orig_q=RN:38074249
46. Barrow MP, Witt M, Headley JV, Peru KM. 2010. Athabasca oil sands process water: characterization by atmospheric pressure photoionization and electrospray ionization Fourier transform ion cyclotron resonance mass spectrometry. *Anal. Chem.* 82(9):3727–35
47. Barrow MP, Peru KM, McMartin DW, Headley JV. 2016. Effects of extraction pH on the Fourier transform ion cyclotron resonance mass spectrometry profiles of Athabasca oil sands process water. *Energy Fuels* 30(5):3615–21
48. Brown LD, Ulrich AC. 2015. Oil sands naphthenic acids: a review of properties, measurement, and treatment. *Chemosphere* 127:276–90
49. Huba AK, Huba K, Gardinali PR. 2016. Understanding the atmospheric pressure ionization of petroleum components: the effects of size, structure, and presence of heteroatoms. *Sci. Total Environ.* 568:1018–25
50. Hertzog J, Carré V, Le Brech Y, Mackay CL, Dufour A, et al. 2017. Combination of electrospray ionization, atmospheric pressure photoionization and laser desorption ionization Fourier transform ion cyclotron resonance mass spectrometry for the investigation of complex mixtures—application to the petroleomic analysis. *Anal. Chim. Acta* 969:26–34
51. Constapel M, Schellenträger M, Schmitz OJ, Gäb S, Brockmann KJ, et al. 2005. Atmospheric-pressure laser ionization: a novel ionization method for liquid chromatography/mass spectrometry. *Rapid Commun. Mass Spectrom.* 19(3):326–36
52. Panda SK, Brockmann K-J, Benter T, Schrader W. 2011. Atmospheric pressure laser ionization (APLI) coupled with Fourier transform ion cyclotron resonance mass spectrometry applied to petroleum samples analysis: comparison with electrospray ionization and atmospheric pressure photoionization methods. *Rapid Commun. Mass Spectrom.* 25(16):2317–26
53. Benigni P, Debord JD, Thompson CJ, Gardinali P, Fernandez-Lima F. 2016. Increasing polyaromatic hydrocarbon (PAH) molecular coverage during fossil oil analysis by combining gas chromatography and atmospheric-pressure laser ionization Fourier transform ion cyclotron resonance mass spectrometry (FT-ICR MS). *Energy Fuels* 30(1):196–203
54. Barrow MP, Peru KM, Headley JV. 2014. An added dimension: GC atmospheric pressure chemical ionization FTICR MS and the Athabasca oil sands. *Anal. Chem.* 86:8281–88
55. Thomas MJ, Collinge E, Witt M, Palacio Lozano DC, Vane CH, et al. 2019. Petroleomic depth profiling of Staten Island salt marsh soil: 2 ω detection FTICR MS offers a new solution for the analysis of environmental contaminants. *Sci. Total Environ.* 662:852–62
56. Palacio Lozano DC, Orrego-Ruiz JA, Barrow MP, Cabanzo Hernandez R, Mejía-Ospino E. 2016. Analysis of the molecular weight distribution of vacuum residues and their molecular distillation fractions by laser desorption ionization mass spectrometry. *Fuel* 171:247–52
57. Pereira TMC, Vanini G, Tose LV, Cardoso FMR, Fleming FP, et al. 2014. FT-ICR MS analysis of asphaltenes: asphaltenes go in, fullerenes come out. *Fuel* 131:49–58
58. Pinkston DS, Duan P, Gallardo VA, Habicht SC, Tan X, et al. 2009. Analysis of asphaltenes and asphaltene model compounds by laser-induced acoustic desorption/Fourier transform ion cyclotron resonance mass spectrometry. *Energy Fuels* 23(11):5564–70
59. Wu C, Qian K, Walters CC, Mennito A. 2015. Application of atmospheric pressure ionization techniques and tandem mass spectrometry for the characterization of petroleum components. *Int. J. Mass Spectrom.* 377(1):728–35
60. Tose LV, Murgu M, Vaz BG, Romão W. 2017. Application of atmospheric solids analysis probe mass spectrometry (ASAP-MS) in petroleomics: analysis of condensed aromatics standards, crude oil, and paraffinic fraction. *J. Am. Soc. Mass Spectrom.* 28(11):2401–7

61. Rodgers RP, Mapolelo MM, Robbins WK, Chacón-Patiño ML, Putman JC, et al. 2019. Combating selective ionization in the high resolution mass spectral characterization of complex mixtures. *Faraday Discuss.* 218:29–51
62. Headley JV, Peru KM, Barrow MP, Derrick PJ. 2007. Characterization of naphthenic acids from Athabasca oil sands using electrospray ionization: the significant influence of solvents. *Anal. Chem.* 79(16):6222–29
63. Smith DF, Podgorski DC, Rodgers RP, Blakney GT, Hendrickson CL. 2018. 21 Tesla FT-ICR mass spectrometer for ultrahigh-resolution analysis of complex organic mixtures. *Anal. Chem.* 90(3):2041–47
64. Shaw JB, Lin T-Y, Leach FE, Tolmachev AV, Tolić N, et al. 2016. 21 Tesla Fourier transform ion cyclotron resonance mass spectrometer greatly expands mass spectrometry toolbox. *J. Am. Soc. Mass Spectrom.* 27(12):1929–36
65. Kostyukevich YI, Vladimirov GN, Nikolaev EN. 2012. Dynamically harmonized FT-ICR cell with specially shaped electrodes for compensation of inhomogeneity of the magnetic field. Computer simulations of the electric field and ion motion dynamics. *J. Am. Soc. Mass Spectrom.* 23(12):2198–207
66. Lioznov A, Baykut G, Nikolaev E. 2019. Analytical solution for the electric field inside dynamically harmonized FT-ICR cell. *J. Am. Soc. Mass Spectrom.* 30(5):778–86
67. Cho E, Witt M, Hur M, Jung M-J, Kim S. 2017. Application of FT-ICR MS equipped with quadrupole detection for analysis of crude oil. *Anal. Chem.* 89(22):12101–7
68. Kim D, Kim S, Son S, Jung M-J, Kim S. 2019. Application of online liquid chromatography 7 T FT-ICR mass spectrometer equipped with quadrupole detection for analysis of natural organic matter. *Anal. Chem.* 91(12):7690–97
69. Schmidt EM, Pudenzi MA, Santos JM, Angolini CFF, Pereira RCL, et al. 2018. Petroleomics via Orbitrap mass spectrometry with resolving power above 1 000 000 at m/z 200. *RSC Adv.* 8(11):6183–91
70. Gaspar A, Schrader W. 2012. Expanding the data depth for the analysis of complex crude oil samples by Fourier transform ion cyclotron resonance mass spectrometry using the spectral stitching method. *Rapid Commun. Mass Spectrom.* 26(9):1047–52
71. Vetere A, Schrader W. 2017. Mass spectrometric coverage of complex mixtures: exploring the carbon space of crude oil. *ChemistrySelect* 2(3):849–53
72. Krajewski LC, Rodgers RP, Marshall AG. 2017. 126 264 Assigned chemical formulas from an atmospheric pressure photoionization 9.4 T Fourier transform positive ion cyclotron resonance mass spectrometer. *Anal. Chem.* 89(21):11318–24
73. Cho E, Park M, Hur M, Kang G, Kim YH, Kim S. 2019. Molecular-level investigation of soils contaminated by oil spilled during the Gulf War. *J. Hazard. Mater.* 373:271–77
74. Afonso C, Chaux C, Davies AN, Delsuc M-A, Fernandez Lima F, et al. 2019. Future challenges and new approaches: general discussion. *Faraday Discuss.* 218:505–23
75. Ledford EB, White RL, Ghaderi S, Wilkins CL, Gross ML. 1980. Coupling of capillary gas chromatograph and Fourier transform mass spectrometer. *Anal. Chem.* 52(14):2450–51
76. Szulejko JE, Solouki T. 2002. Potential analytical applications of interfacing a GC to an FT-ICR MS: fingerprinting complex sample matrixes. *Anal. Chem.* 74(14):3434–42
77. Rügner CP, Schwemer T, Sklorz M, O'Connor PB, Barrow MP, Zimmermann R. 2017. Comprehensive chemical comparison of fuel composition and aerosol particles emitted from a ship diesel engine by gas chromatography atmospheric pressure chemical ionisation ultra-high resolution mass spectrometry with improved data processing routines. *Eur. J. Mass Spectrom.* 23(1):28–39
78. Schwemer T, Rügner CP, Sklorz M, Zimmermann R. 2015. Gas chromatography coupled to atmospheric pressure chemical ionization FT-ICR mass spectrometry for improvement of data reliability. *Anal. Chem.* 87(24):11957–61
79. Kondyli A, Schrader W. 2019. High-resolution GC/MS studies of a light crude oil fraction. *J. Mass Spectrom.* 54(1):47–54
80. Hawkes JA, Sjöberg PJR, Bergquist J, Tranvik LJ. 2019. Complexity of dissolved organic matter in the molecular size dimension: insights from coupled size exclusion chromatography electrospray ionisation mass spectrometry. *Faraday Discuss.* 218:52–71

81. Pereira AS, Martin JW. 2015. Exploring the complexity of oil sands process-affected water by high efficiency supercritical fluid chromatography/Orbitrap mass spectrometry. *Rapid Commun. Mass Spectrom.* 29(8):735–44
82. Silveira JA, Michelmann K, Ridgeway ME, Park MA. 2016. Fundamentals of trapped ion mobility spectrometry part II: fluid dynamics. *J. Am. Soc. Mass Spectrom.* 27(4):585–95
83. Santos JM, Galaverna RS, Pudenzi MA, Schmidt EM, Sanders NL, et al. 2015. Petroleomics by ion mobility mass spectrometry: resolution and characterization of contaminants and additives in crude oils and petrofuels. *Anal. Methods* 7(11):4450–63
84. Lalli PM, Klitzke F, Corilo YE, Pudenzi MA, Pereira RCL, et al. 2013. Petroleomics by traveling wave ion mobility–mass spectrometry using CO₂ as a drift gas. *Energy Fuels* 27(12):7277–86
85. Benigni P, Fernandez-Lima F. 2016. Oversampling selective accumulation trapped ion mobility spectrometry coupled to FT-ICR MS: fundamentals and applications. *Anal. Chem.* 88(14):7404–12
86. Tose LV, Benigni P, Leyva D, Sundberg A, Ramírez CE, et al. 2018. Coupling trapped ion mobility spectrometry to mass spectrometry: trapped ion mobility spectrometry–time-of-flight mass spectrometry versus trapped ion mobility spectrometry–Fourier transform ion cyclotron resonance mass spectrometry. *Rapid Commun. Mass Spectrom.* 32(15):1287–95
87. Benigni P, Sandoval K, Thompson CJ, Ridgeway ME, Park MA, et al. 2017. Analysis of photoirradiated water accommodated fractions of crude oils using tandem TIMS and FT-ICR MS. *Environ. Sci. Technol.* 51(11):5978–88
88. Rüger CP, Maillard J, Le Maître J, Ridgeway M, Thompson CJ, et al. 2019. Structural study of analogues of Titan’s haze by trapped ion mobility coupled with a Fourier transform ion cyclotron mass spectrometer. *J. Am. Soc. Mass Spectrom.* 30(7):1169–73
89. Zahraei A, Arisz PWF, van Bavel AP, Heeren RMA. 2018. Evaluation of thin-layer chromatography–laser desorption ionization Fourier transform ion cyclotron resonance mass spectrometric imaging for visualization of crude oil interactions. *Energy Fuels* 32(7):7347–57
90. Koch BP, Dittmar T. 2006. From mass to structure: an aromaticity index for high-resolution mass data of natural organic matter. *Rapid Commun. Mass Spectrom.* 20(5):926–32
91. Koch BP, Dittmar T. 2016. Erratum. From mass to structure: an aromaticity index for high-resolution mass data of natural organic matter. *Rapid Commun. Mass Spectrom.* 30(1):250
92. Zhu Y, Vieth-Hillebrand A, Noah M, Poetz S. 2019. Molecular characterization of extracted dissolved organic matter from New Zealand coals identified by ultrahigh resolution mass spectrometry. *Int. J. Coal Geol.* 203:74–86
93. Stubbins A, Spencer RGM, Chen H, Hatcher PG, Mopper K, et al. 2010. Illuminated darkness: molecular signatures of Congo River dissolved organic matter and its photochemical alteration as revealed by ultrahigh precision mass spectrometry. *Limnol. Oceanogr.* 55(4):1467–77
94. Zhurov KO, Kozhinov AN, Tsybin YO. 2013. Hexagonal class representation for fingerprinting and facile comparison of petroleomic samples. *Anal. Chem.* 85(11):5311–15
95. Gatto L, Breckels LM, Naake T, Gibb S. 2015. Visualization of proteomics data using R and bioconductor. *Proteomics* 15(8):1375–89
96. Kew W, Blackburn JWT, Clarke DJ, Uhrin D. 2017. Interactive van Krevelen diagrams—advanced visualisation of mass spectrometry data of complex mixtures. *Rapid Commun. Mass Spectrom.* 31(7):658–62
97. Leefmann T, Frickenhaus S, Koch BP. 2018. UltraMassExplorer: a browser-based application for the evaluation of high-resolution mass spectrometric data. *Rapid Commun. Mass Spectrom.* 33:193–202
98. Kind T, Fiehn O. 2007. Seven Golden Rules for heuristic filtering of molecular formulas obtained by accurate mass spectrometry. *BMC Bioinform.* 8(1):105
99. Afonso C, Barrow MP, Davies AN, Delsuc M-A, Ebbels T, et al. 2019. Data mining and visualisation: general discussion. *Faraday Discuss.* 218:354–71
100. Barrow MP, Headley JV, Derrick PJ. 2009. Data visualization for the characterization of naphthenic acids within petroleum samples data visualization for the characterization of naphthenic acids within petroleum samples. *Energy Fuels* 23(12):2592–99

101. Palacio Lozano DC, Orrego-Ruiz JA, Cabanzo Hernández R, Guerrero JE, Mejía-Ospino E. 2017. APPI(+)-FTICR mass spectrometry coupled to partial least squares with genetic algorithm variable selection for prediction of API gravity and CCR of crude oil and vacuum residues. *Fuel* 193:39–44
102. Hur M, Ware RL, Park J, McKenna AM, Rodgers RP, et al. 2018. Statistically significant differences in composition of petroleum crude oils revealed by volcano plots generated from ultrahigh resolution Fourier transform ion cyclotron resonance mass spectra. *Energy Fuels* 32(2):1206–12
103. Gavard R, Rossell D, Spencer SEF, Barrow MP. 2017. Themis: batch preprocessing for ultrahigh-resolution mass spectra of complex mixtures. *Anal. Chem.* 89(21):11383–90
104. Cho Y, Ahmed A, Islam A, Kim S. 2015. Developments in FT-ICR MS instrumentation, ionization techniques, and data interpretation methods for petroleomics. *Mass Spectrom. Rev.* 34:248–63
105. Silva SL, Silva AMS, Ribeiro JC, Martins FG, Da Silva FA, Silva CM. 2011. Chromatographic and spectroscopic analysis of heavy crude oil mixtures with emphasis in nuclear magnetic resonance spectroscopy: a review. *Anal. Chim. Acta* 707(1–2):18–37
106. Speight JG. 2006. *The Chemistry and Technology of Petroleum*. Boca Raton, FL: CRC Press. 4th ed.
107. Shaw JM, Satyro MA, Yarranton HW. 2017. Phase behavior and properties of heavy oils. In *Springer Handbook of Petroleum Technology*, ed. CS Hsu, PR Robinson, pp. 273–318. Cham, Switz.: Springer
108. Gaspar A, Zellermann E, Lababidi S, Reece J, Schrader W. 2012. Characterization of saturates, aromatic, resins, and asphaltenes heavy crude oil fractions by atmospheric pressure laser ionization Fourier transform ion cyclotron resonance mass spectrometry. *Energy Fuels* 26:3481–87
109. Cho Y, Na J, Nho N, Kim S, Kim S. 2012. Application of saturates, aromatics, resins, and asphaltenes crude oil fractionation for detailed chemical characterization of heavy crude oils by Fourier transform ion cyclotron resonance mass spectrometry equipped with atmospheric pressure photoionization. *Energy Fuels* 26(5):2558–65
110. Hur M, Yeo I, Kim E, No M, Koh J, et al. 2010. Correlation of FT-ICR mass spectra with the chemical and physical properties of associated crude oils. *Energy Fuels* 24(10):5524–32
111. Hsu CS, Dechert GJ, Robbins WK, Fukuda EK. 2000. Naphthenic acids in crude oils characterized by mass spectrometry. *Energy Fuels* 14(1):217–23
112. Mapolelo MM, Rodgers RP, Blakney GT, Yen AT, Asomaning S, Marshall AG. 2011. Characterization of naphthenic acids in crude oils and naphthenates by electrospray ionization FT-ICR mass spectrometry. *Int. J. Mass Spectrom.* 300(2–3):149–57
113. Ren L, Wu J, Qian Q, Liu X, Meng X, et al. 2019. Separation and characterization of sulfoxides in crude oils. *Energy Fuels* 33(2):796–804
114. Liu L, Song C, Tian S, Zhang Q, Cai X, et al. 2019. Structural characterization of sulfur-containing aromatic compounds in heavy oils by FT-ICR mass spectrometry with a narrow isolation window. *Fuel* 240:40–48
115. Panda SK, Alawani NA, Lajami AR, Al-Qunaysi TA, Muller H. 2019. Characterization of aromatic hydrocarbons and sulfur heterocycles in Saudi Arabian heavy crude oil by gel permeation chromatography and ultrahigh resolution mass spectrometry. *Fuel* 235:1420–26
116. Fink J. 2016. Processes. In *Guide to the Practical Use of Chemicals in Refineries and Pipelines*, ed. J Fink, pp. 185–223. Boston: Gulf Prof.
117. Gutiérrez Sama S, Barrère-Mangote C, Bouyssière B, Giusti P, Lobinski R. 2018. Recent trends in element speciation analysis of crude oils and heavy petroleum fractions. *Trends Anal. Chem.* 104:69–76
118. Javadli R, de Klerk A. 2012. Desulfurization of heavy oil. *Appl. Petrochem. Res.* 1(1):3–19
119. Panda SK, Schrader W, Al-Hajji A, Andersson JT. 2007. Distribution of polycyclic aromatic sulfur heterocycles in three Saudi Arabian crude oils as determined by Fourier transform ion cyclotron resonance mass spectrometry. *Energy Fuels* 21(2):1071–77
120. Akbarzadeh K, Zhang D, Creek J, Jamaluddin AJ, Marshall AG, et al. 2007. Asphaltenes—problematic but rich in potential. *Oilf. Rev.* 19(2):22–43
121. Buckley JS, Wang J, Creek JL. 2007. Solubility of the least-soluble asphaltenes. In *Asphaltenes, Heavy Oils, and Petroleomics*, ed. OC Mullins, EY Sheu, A Hammami, AG Marshall, pp. 401–37. New York: Springer
122. Wiehe IA, Kennedy RJ. 2000. Oil compatibility model and crude oil incompatibility. *Energy Fuels* 14(1):56–59

123. Dickie JP, Yen TF. 1967. Macrostructures of the asphaltic fractions by various instrumental methods. *Anal. Chem.* 39(14):1847–52
124. Mullins OC. 2011. The asphaltenes. *Annu. Rev. Anal. Chem.* 4:393–418
125. Mullins OC, Sabbah H, Pomerantz AE, Barre L, Andrews AB, et al. 2012. Advances in asphaltene science and the Yen–Mullins model. *Energy Fuels* 26:3986–4003
126. Tang W, Hurt MR, Sheng H, Riedeman JS, Borton DJ, et al. 2015. Structural comparison of asphaltenes of different origins using multi-stage tandem mass spectrometry. *Energy Fuels* 29(3):1309–14
127. Nyadong L, Lai J, Thompsen C, Lafrancois CJ, Cai X, et al. 2018. High-field Orbitrap mass spectrometry and tandem mass spectrometry for molecular characterization of asphaltenes. *Energy Fuels* 32(1):294–305
128. Chacón-Patiño ML, Rowland SM, Rodgers RP. 2018. Advances in asphaltene petroleomics. Part 3. Dominance of island or archipelago structural motif is sample dependent. *Energy Fuels* 32(9):9106–20
129. Yim UH, Kim M, Ha SY, Kim S, Shim WJ. 2012. Oil spill environmental forensics: the Hebei spirit oil spill case. *Environ. Sci. Technol.* 46(12):6431–37
130. Barron M. 2019. *Long term ecological impacts of oil spills: comparison of Exxon Valdez, Hebei Spirit and Deepwater Horizon*. Presented at the Alaska Marine Science Symposium, Pensacola Beach, FL, Jan. 28–Feb. 1. https://cfpub.epa.gov/si/si_public_record_report.cfm?Lab=NHEERL&dirEntryId=344266
131. Aepli C, Carmichael CA, Nelson RK, Lemkau KL, Graham WM, et al. 2012. Oil weathering after the Deepwater Horizon disaster led to the formation of oxygenated residues. *Environ. Sci. Technol.* 46(16):8799–807
132. Ray PZ, Chen H, Podgorski DC, McKenna AM, Tarr MA. 2014. Sunlight creates oxygenated species in water-soluble fractions of Deepwater Horizon oil. *J. Hazard. Mater.* 280:636–43
133. Griffiths MT, Da Campo R, O'Connor PB, Barrow MP. 2014. Throwing light on petroleum: simulated exposure of crude oil to sunlight and characterization using atmospheric pressure photoionization Fourier transform ion cyclotron resonance mass spectrometry. *Anal. Chem.* 86(1):527–34
134. Chen H, Hou A, Corilo YE, Lin Q, Lu J, et al. 2016. 4 Years after the deepwater horizon spill: molecular transformation of Macondo well oil in Louisiana salt marsh sediments revealed by FT-ICR mass spectrometry. *Environ. Sci. Technol.* 50(17):9061–69
135. Sørensen L, McCormack P, Altin D, Robson WJ, Booth AM, et al. 2019. Establishing a link between composition and toxicity of offshore produced waters using comprehensive analysis techniques—A way forward for discharge monitoring? *Sci. Total Environ.* 694:133682
136. Headley JV, Peru KM, Barrow MP. 2016. Advances in mass spectrometric characterization of naphthenic acids fraction compounds in oil sands environmental samples and crude oil—a review. *Mass Spectrom. Rev.* 35:311–28
137. Yi Y, Han J, Jean Birks S, Borchers CH, Gibson JJ. 2017. Profiling of dissolved organic compounds in the oil sands region using complimentary liquid-liquid extraction and ultrahigh resolution Fourier transform mass spectrometry. *Environ. Earth Sci.* 76(24):828
138. Barrow MP, Peru KM, Headley JV. 2014. An added dimension: GC atmospheric pressure chemical ionization FTICR MS and the Athabasca oil sands. *Anal. Chem.* 86(16):8281–88
139. Bauer AE, Hewitt LM, Parrott JL, Bartlett AJ, Gillis PL, et al. 2019. The toxicity of organic fractions from aged oil sands process-affected water to aquatic species. *Sci. Total Environ.* 669:702–10
140. Marentette JR, Frank RA, Bartlett AJ, Gillis PL, Hewitt LM, et al. 2015. Toxicity of naphthenic acid fraction components extracted from fresh and aged oil sands process-affected waters, and commercial naphthenic acid mixtures, to fathead minnow (*Pimephales promelas*) embryos. *Aquat. Toxicol.* 164:108–17
141. Smith EA, Lee YJ. 2010. Petroleomic analysis of bio-oils from the fast pyrolysis of biomass: laser desorption ionization-linear ion trap-orbitrap mass spectrometry approach. *Energy Fuels* 24(9):5190–98
142. Miettinen I, Mäkinen M, Vilppo T, Jänis J. 2015. Compositional characterization of phase-separated pine wood slow pyrolysis oil by negative-ion electrospray ionization Fourier transform ion cyclotron resonance mass spectrometry. *Energy Fuels* 29(3):1758–65
143. Rivas-Ubach A, Liu Y, Bianchi TS, Tolić N, Jansson C, Paša-Tolić L. 2018. Moving beyond the van Krevelen diagram: a new stoichiometric approach for compound classification in organisms. *Anal. Chem.* 90(10):6152–60

144. Podgorski DC, Hamdan R, McKenna AM, Nyadong L, Rodgers RP, et al. 2012. Characterization of pyrogenic black carbon by desorption atmospheric pressure photoionization Fourier transform ion cyclotron resonance mass spectrometry. *Anal. Chem.* 84(3):1281–87
145. Kostyukevich Y, Kononikhin A, Popov I, Kharybin O, Perminova I, et al. 2013. Enumeration of labile hydrogens in natural organic matter by use of hydrogen/deuterium exchange Fourier transform ion cyclotron resonance mass spectrometry. *Anal. Chem.* 85(22):11007–13
146. Zito P, Podgorski DC, Johnson J, Chen H, Rodgers RP, et al. 2019. Molecular-level composition and acute toxicity of photosolubilized petrogenic carbon. *Environ. Sci. Technol.* 53(14):8235–43
147. Hawkes JA, Patriarca C, Sjöberg PJR, Tranvik LJ, Bergquist J. 2018. Extreme isomeric complexity of dissolved organic matter found across aquatic environments. *Limnol. Oceanogr. Lett.* 3(2):21–30
148. Gutiérrez Sama S, Farenc M, Barrère-Mangote C, Lobinski R, Afonso C, et al. 2018. Molecular fingerprints and speciation of crude oils and heavy fractions revealed by molecular and elemental mass spectrometry: keystone between petroleomics, metallopetroleomics, and petrointeractomics. *Energy Fuels* 32(4):4593–605
149. Niyonsaba E, Manheim JM, Yerabolu R, Kenttämäa HI. 2019. Recent advances in petroleum analysis by mass spectrometry. *Anal. Chem.* 91(1):156–77
150. Vetere A, Alachraf MW, Panda SK, Andersson JT, Schrader W. 2018. Studying the fragmentation mechanism of selected components present in crude oil by collision-induced dissociation mass spectrometry. *Rapid Commun. Mass Spectrom.* 32(24):2141–51